

Double hybrid density-functional theory using the Coulomb-attenuating method

Yann Cornaton*, Emmanuel Fromager†

March 19, 2014

Abstract

A double hybrid approximation using the Coulomb-attenuating method (CAM-DH) is derived within range-separated density-functional perturbation theory, in the spirit of a recent work by Cornaton *et al.* [Phys. Rev. A 88, 022516 (2013)]. The energy expression recovered through second order is linear in the parameters α and β that control the Coulomb attenuation. The method has been tested within the local density approximation on a small test set consisting of rare-gas and alkaline-earth-metal dimers as well as diatomics with single, double and triple bonds. In this context, the semi-empirical $\alpha = 0.19$ and $\beta = 0.46$ parameters, that were optimized for the hybrid CAM-B3LYP functional, do not provide accurate interaction and total energies. Using semi-local functionals with density scaling, that was neglected in this work, may lead to different conclusions. Calibration studies on a larger test set would be necessary at this point. This is left for future work. Finally, we propose as a perspective an alternative CAM-DH approach that relies on the perturbation expansion of a partially long-range interacting wavefunction. In this case the energy is not linear anymore in α and β . Work is in progress in this direction.

*Center for Theoretical and Computational Chemistry, Department of Chemistry, Universitetet i Tromsø, Tromsø, Norway

†Laboratoire de Chimie Quantique, Institut de Chimie, CNRS/Université de Strasbourg, Strasbourg, France

1 INTRODUCTION

The combination of density-functional theory (DFT) with second-order Møller–Plesset (MP2) perturbation theory can be achieved rigorously when splitting the electron-electron repulsion into two complementary contributions^{1–6}. Note that, even though we focus here on MP2, various correlated methods have been merged with DFT along those lines (see Ref.⁷ and the references therein). The resulting MP2-DFT energy expressions are usually referred to as double hybrid approximations. So far two separations of the two-electron interaction have been investigated: one is simply linear⁴ and the other one is based on the range of the interaction, thus leading to the so-called long-range/short-range separation⁸.

These separations have also been used in conventional (single determinantal) hybrid DFT for the purpose of improving the description of the exchange energy. While the linear separation underlies popular hybrid functionals such as the Becke three-parameter Lee-Yang-Parr functional (B3LYP)⁹, standard long-range-corrected hybrid DFT (LC-DFT)¹⁰ uses the range separation based on the error function. The combination of the two latter approaches lead to the Coulomb-attenuated method based on the B3LYP functional (CAM-B3LYP)¹¹. While preserving the accuracy of B3LYP for ground-state properties, CAM-B3LYP became popular for the computation of charge-transfer excitations within time-dependent DFT¹².

We explore in this work rigorous double hybrid extensions for CAM-B3LYP with the purpose of improving both exchange and correlation ground-state energies. The paper is organized as follows: In Sec. 2 the theory underlying Coulomb-attenuating double hybrid DFT is presented. The latter will be based on the perturbation expansion of a fully long-range interacting wavefunction. Computational details are then given in Sec. 3 and results obtained on a small test set, consisting of rare-gas and alkaline-earth-metal dimers as well as diatomics with single, double and triple bonds, are discussed in Sec. 4. As a perspective, we finally propose in Sec. 5 an alternative formulation that relies on a partially long-range-interacting wavefunction. Conclusions are given in Sec. 6.

2 THEORY

In this section we present the theory underlying the construction of CAM-DH approximations. It is organized as follows: For pedagogical purposes, standard hybrid LC-DFT and range-separated double hybrid DFT are introduced in Sec. 2.1. We then discuss the multi-determinantal extension of standard hybrid CAM-DFT in Sec. 2.2. In Sec. 2.3 we consider a double adiabatic connection and apply scaling relations in order to derive implementable expressions for complement density-functional correlation energies. A CAM-DH energy expression is finally derived in Sec. 2.4.

2.1 Hybrid and double hybrid DFT based on range separation

2.1.1 Long-range corrected hybrid DFT

According to the Hohenberg–Kohn theorems¹³, the exact ground-state energy of an electronic system can be expressed as

$$E = \min_n \left\{ F[n] + \int d\mathbf{r} v_{\text{ne}}(\mathbf{r}) n(\mathbf{r}) \right\}, \quad (1)$$

where $v_{\text{ne}}(\mathbf{r})$ is the nuclear potential and $F[n]$ denotes the universal Levy–Lieb (LL) functional^{14,15}

$$F[n] = \min_{\Psi \rightarrow n} \langle \Psi | \hat{T} + \hat{W}_{\text{ee}} | \Psi \rangle. \quad (2)$$

\hat{T} is the kinetic energy operator and \hat{W}_{ee} denotes the regular two-electron interaction operator with $w_{\text{ee}}(r_{12}) = 1/r_{12}$. The minimization in Eq. (2) is restricted to wavefunctions with density n .

In standard hybrid LC-DFT¹⁰, the following partitioning of the LL functional is used

$$F[n] = \left(\min_{\Phi \rightarrow n} \langle \Phi | \hat{T} + \hat{W}_{\text{ee}}^{\text{lr},\mu} | \Phi \rangle \right) + E_{\text{H}}^{\text{sr},\mu}[n] + E_{\text{x}}^{\text{sr},\mu}[n] + U_{\text{c}}^{\mu}[n], \quad (3)$$

where the minimization in the first term on the right-hand side of Eq. (3) is restricted to single determinants Φ with density n , $\hat{W}_{ee}^{\text{lr},\mu}$ is the long-range electron-electron interaction operator defined by $w_{ee}^{\text{lr},\mu}(r_{12}) = \text{erf}(\mu r_{12})/r_{12}$ and $E_{\text{H}}^{\text{sr},\mu}[n] = 1/2 \int \int d\mathbf{r}_1 d\mathbf{r}_2 n(\mathbf{r}_1)n(\mathbf{r}_2) w_{ee}^{\text{sr},\mu}(r_{12})$ denotes the short-range Hartree density functional with $w_{ee}^{\text{sr},\mu}(r_{12}) = \text{erfc}(\mu r_{12})/r_{12}$. In this scheme the range separation is controlled by the μ parameter. Note that, for $\mu = 0$, the long-range interaction equals zero and the short-range interaction reduces to the regular two-electron interaction $1/r_{12}$, thus leading to the standard Kohn–Sham (KS) decomposition¹⁶

$$F[n] = T_{\text{s}}[n] + E_{\text{H}}[n] + E_{\text{x}}[n] + E_{\text{c}}[n], \quad (4)$$

where $T_{\text{s}}[n] = \langle \Phi^{\text{KS}}[n] | \hat{T} | \Phi^{\text{KS}}[n] \rangle$ is the non-interacting kinetic energy functional and $\Phi^{\text{KS}}[n]$ denotes the KS determinant with density n . The latter enables to define the exact short-range exchange energy in Eq. (3) as

$$E_{\text{x}}^{\text{sr},\mu}[n] = \langle \Phi^{\text{KS}}[n] | \hat{W}_{ee}^{\text{sr},\mu} | \Phi^{\text{KS}}[n] \rangle - E_{\text{H}}^{\text{sr},\mu}[n], \quad (5)$$

which gives the following expression for the *exact* complement correlation functional

$$U_{\text{c}}^{\mu}[n] = E_{\text{c}}[n] + \langle \Phi^{\text{KS}}[n] | \hat{T} + \hat{W}_{ee}^{\text{lr},\mu} | \Phi^{\text{KS}}[n] \rangle - \min_{\Phi \rightarrow n} \langle \Phi | \hat{T} + \hat{W}_{ee}^{\text{lr},\mu} | \Phi \rangle. \quad (6)$$

Combining Eq. (1) with Eq. (3) leads to the following expression for the exact ground-state energy

$$E = \min_{\Phi} \left\{ \langle \Phi | \hat{T} + \hat{V}_{\text{ne}} + \hat{W}_{ee}^{\text{lr},\mu} | \Phi \rangle + E_{\text{H}}^{\text{sr},\mu}[n_{\Phi}] + E_{\text{x}}^{\text{sr},\mu}[n_{\Phi}] + U_{\text{c}}^{\mu}[n_{\Phi}] \right\}, \quad (7)$$

where the nuclear potential operator equals $\hat{V}_{\text{ne}} = \int d\mathbf{r} v_{\text{ne}}(\mathbf{r}) \hat{n}(\mathbf{r})$ and $\hat{n}(\mathbf{r}) = \sum_{\sigma=\alpha,\beta} \hat{\Psi}_{\sigma}^{\dagger}(\mathbf{r}) \hat{\Psi}_{\sigma}(\mathbf{r})$ is the density operator written in second quantized form. Note that, in practical calculations, $U_{\text{c}}^{\mu}[n]$ is simply replaced by the regular correlation functional $E_{\text{c}}[n]$ since the last two terms on the right-hand side of Eq. (6) are expected to be relatively close, like in conventional hybrid DFT¹⁷. Let us stress that in hybrid LC-DFT, range separation is only used for the exchange energy. The correlation energy is, like in KS-DFT, described by a density functional. Consequently one single determinant is sufficient for computing the ground-state energy. The latter becomes *exact* when both exact short-range exchange and complement correlation functionals are used.

2.1.2 Multi-determinant range-separated DFT

In order to improve the description of the long-range correlation energy in approximate LC-DFT schemes, Savin has proposed⁸ a multi-determinantal extension of Eq. (7) based on the following decomposition of the LL functional:

$$\begin{aligned} F[n] &= \left(\min_{\Psi \rightarrow n} \langle \Psi | \hat{T} + \hat{W}_{ee}^{\text{lr},\mu} | \Psi \rangle \right) + E_{\text{Hxc}}^{\text{sr},\mu}[n] \\ &= \langle \Psi^\mu[n] | \hat{T} + \hat{W}_{ee}^{\text{lr},\mu} | \Psi^\mu[n] \rangle + E_{\text{Hxc}}^{\text{sr},\mu}[n], \end{aligned} \quad (8)$$

where the complement μ -dependent short-range Hartree-exchange-correlation (srHxc) density-functional energy is denoted $E_{\text{Hxc}}^{\text{sr},\mu}[n]$. Note that, in contrast to hybrid LC-DFT (see Eq. (3)), the minimization in the first term on the right-hand side of Eq. (8) is *not* restricted to single determinants. Consequently, the minimizing wavefunction $\Psi^\mu[n]$ with density n is *multi-determinantal*. In other words, purely long-range correlation effects are now treated explicitly, in wavefunction theory. Note that the LL universal functional expression in Eq. (2) is recovered from Eq. (8) in the $\mu \rightarrow +\infty$ limit. The exact short-range exchange energy is usually defined, like in hybrid LC-DFT, from the KS determinant thus leading to the following expression for the srHxc energy:

$$\begin{aligned} E_{\text{Hxc}}^{\text{sr},\mu}[n] &= E_{\text{H}}^{\text{sr},\mu}[n] + E_{\text{x}}^{\text{sr},\mu}[n] + E_{\text{c}}^{\text{sr},\mu}[n] \\ &= \langle \Phi^{\text{KS}}[n] | \hat{W}_{ee}^{\text{sr},\mu} | \Phi^{\text{KS}}[n] \rangle + E_{\text{c}}^{\text{sr},\mu}[n], \end{aligned} \quad (9)$$

where, according to Eqs. (4) and (8), the complement short-range correlation energy can be expressed as

$$\begin{aligned} E_{\text{c}}^{\text{sr},\mu}[n] &= T_{\text{s}}[n] + E_{\text{H}}[n] - E_{\text{H}}^{\text{sr},\mu}[n] + E_{\text{x}}[n] - E_{\text{x}}^{\text{sr},\mu}[n] + E_{\text{c}}[n] \\ &\quad - \left(\min_{\Psi \rightarrow n} \langle \Psi | \hat{T} + \hat{W}_{ee}^{\text{lr},\mu} | \Psi \rangle \right). \end{aligned} \quad (10)$$

By using the KS decomposition of the long-range interacting LL functional,

$$\min_{\Psi \rightarrow n} \langle \Psi | \hat{T} + \hat{W}_{ee}^{\text{lr},\mu} | \Psi \rangle = T_{\text{s}}[n] + \langle \Phi^{\text{KS}}[n] | \hat{W}_{ee}^{\text{lr},\mu} | \Phi^{\text{KS}}[n] \rangle + E_{\text{c}}^{\text{lr},\mu}[n], \quad (11)$$

where $E_{\text{c}}^{\text{lr},\mu}[n]$ denotes the purely long-range density-functional correlation energy, we obtain the compact expression

$$E_{\text{c}}^{\text{sr},\mu}[n] = E_{\text{c}}[n] - E_{\text{c}}^{\text{lr},\mu}[n]. \quad (12)$$

Local density approximations (LDA) to the short-range correlation functional have been developed along those lines when substituting $w_{ee}^{\text{lr},\mu}(r_{12})$ for $1/r_{12}$ in the uniform electron gas model^{18,19}.

Returning to the exact theory, combining Eq. (1) with Eq. (8) leads to

$$\begin{aligned} E &= \min_{\Psi} \left\{ \langle \Psi | \hat{T} + \hat{V}_{\text{ne}} + \hat{W}_{ee}^{\text{lr},\mu} | \Psi \rangle + E_{\text{Hxc}}^{\text{sr},\mu}[n_{\Psi}] \right\} \\ &= \langle \Psi^{\mu} | \hat{T} + \hat{V}_{\text{ne}} + \hat{W}_{ee}^{\text{lr},\mu} | \Psi^{\mu} \rangle + E_{\text{Hxc}}^{\text{sr},\mu}[n_{\Psi^{\mu}}], \end{aligned} \quad (13)$$

where the exact minimizing wavefunction Ψ^{μ} is multi-determinantal due to the explicit description of the long-range interaction. As discussed further in Sec. 2.1.3, applying MP2 in this context leads to the formulation of range-separated double hybrid approximations.

We should finally stress that the decomposition in Eq. (9) is *not* unique. As mentioned in previous works^{20–22}, it seems natural in this context to use the multi-determinantal (md) long-range interacting wavefunction $\Psi^{\mu}[n]$ with density n rather than the KS determinant for the separation of short-range exchange and correlation energies:

$$E_{\text{Hxc}}^{\text{sr},\mu}[n] = \langle \Psi^{\mu}[n] | \hat{W}_{ee}^{\text{sr},\mu} | \Psi^{\mu}[n] \rangle + E_{\text{c,md}}^{\text{sr},\mu}[n]. \quad (14)$$

An adapted complement short-range correlation functional, denoted $E_{\text{c,md}}^{\text{sr},\mu}[n]$, must be used rather than the usual short-range correlation functional $E_{\text{c}}^{\text{sr},\mu}[n]$ in order to recover the same srHxc energy from both decompositions:

$$E_{\text{c,md}}^{\text{sr},\mu}[n] = E_{\text{c}}^{\text{sr},\mu}[n] + \langle \Phi^{\text{KS}}[n] | \hat{W}_{ee}^{\text{sr},\mu} | \Phi^{\text{KS}}[n] \rangle - \langle \Psi^{\mu}[n] | \hat{W}_{ee}^{\text{sr},\mu} | \Psi^{\mu}[n] \rangle. \quad (15)$$

In this work, the LDA-type short-range md correlation functional of Paziani *et al.*¹⁹ will be used.

Returning to the exact theory, since⁷ $\Psi^{\mu}[n_{\Psi^{\mu}}] = \Psi^{\mu}$, combining Eq. (13) with Eq. (14) leads to the alternative range-separated expression for the ground-state energy,

$$E = \langle \Psi^{\mu} | \hat{T} + \hat{V}_{\text{ne}} + \hat{W}_{ee} | \Psi^{\mu} \rangle + E_{\text{c,md}}^{\text{sr},\mu}[n_{\Psi^{\mu}}], \quad (16)$$

where long- and short-range interactions have been recombined.

2.1.3 Range-separated double hybrids

As shown in Refs. ^{1,3,7,23,24}, rigorous range-separated double hybrid (RSDH) energy expressions can be derived from Eqs. (13) and (16) by expanding the multi-determinantal wavefunction Ψ^μ in a self-consistent MP2-type density-functional perturbation theory. Key ideas are the following: By analogy with the regular Hartree–Fock (HF) approximation, the minimization in Eq. (13) is first restricted to single determinantal wavefunctions Φ ,

$$\begin{aligned} E_{\text{HF}}^{\text{srDFT}} &= \min_{\Phi} \left\{ \langle \Phi | \hat{T} + \hat{W}_{\text{ee}}^{\text{lr},\mu} + \hat{V}_{\text{ne}} | \Phi \rangle + E_{\text{Hxc}}^{\text{sr},\mu}[n_{\Phi}] \right\} \\ &= \langle \Phi_0^\mu | \hat{T} + \hat{W}_{\text{ee}}^{\text{lr},\mu} + \hat{V}_{\text{ne}} | \Phi_0^\mu \rangle + E_{\text{Hxc}}^{\text{sr},\mu}[n_{\Phi_0^\mu}], \end{aligned} \quad (17)$$

thus defining the HF-short-range DFT (HF-srDFT) approximation. The minimizing determinant Φ_0^μ , referred to as HF-srDFT determinant, fulfills the following HF-type equation:

$$\left(\hat{T} + \hat{U}_{\text{HF}}^{\text{lr},\mu} + \hat{V}_{\text{ne}} + \int d\mathbf{r} \frac{\delta E_{\text{Hxc}}^{\text{sr},\mu}}{\delta n(\mathbf{r})}[n_{\Phi_0^\mu}] \hat{n}(\mathbf{r}) \right) |\Phi_0^\mu\rangle = \mathcal{E}_0^\mu |\Phi_0^\mu\rangle, \quad (18)$$

where $\hat{U}_{\text{HF}}^{\text{lr},\mu}$ is the long-range analogue of the HF potential operator calculated with the occupied HF-srDFT orbitals. We then introduce a perturbation strength ϵ and define the auxiliary energy¹

$$E^{\epsilon,\mu} = \min_{\Psi} \left\{ \langle \Psi | \hat{T} + \hat{V}_{\text{ne}} + (1 - \epsilon) \hat{U}_{\text{HF}}^{\text{lr},\mu} + \epsilon \hat{W}_{\text{ee}}^{\text{lr},\mu} | \Psi \rangle + E_{\text{Hxc}}^{\text{sr},\mu}[n_{\Psi}] \right\}. \quad (19)$$

Note that, according to Eq. (13), the *exact* ground-state energy is recovered when $\epsilon = 1$. As discussed in details in Refs. ^{1,3,23,24}, the minimizing wavefunction $\Psi^{\epsilon,\mu}$ in Eq. (19) and its density $n_{\Psi^{\epsilon,\mu}}$ can be expanded through second order in the long-range fluctuation potential $\hat{W}_{\text{ee}}^{\text{lr},\mu} - \hat{U}_{\text{HF}}^{\text{lr},\mu}$ as follows,

$$|\Psi^{\epsilon,\mu}\rangle = |\Phi_0^\mu\rangle + \epsilon |\Psi^{(1)\text{lr},\mu}\rangle + \epsilon^2 |\Psi^{(2)\mu}\rangle + \mathcal{O}(\epsilon^3), \quad (20)$$

where the first-order contribution is the long-range analogue of the MP1 wavefunction correction, and

$$n_{\Psi^{\epsilon,\mu}}(\mathbf{r}) = n_{\Phi_0^\mu}(\mathbf{r}) + \epsilon^2 \delta n^{(2)\mu}(\mathbf{r}) + \mathcal{O}(\epsilon^3). \quad (21)$$

Since the density remains unchanged through first order, the auxiliary energy is simply expanded through second order as^{1,3}

$$E^{\epsilon,\mu} = E^{(0)\mu} + \epsilon E^{(1)\mu} + \epsilon^2 E_{\text{MP}}^{(2)\text{lr},\mu} + \mathcal{O}(\epsilon^3), \quad (22)$$

where, when considering the $\epsilon = 1$ limit, the HF-srDFT energy is recovered through first order,

$$E^{(0)\mu} + E^{(1)\mu} = E_{\text{HF}}^{\text{srDFT}}, \quad (23)$$

and the second-order correction to the energy is the purely long-range MP2 correlation energy calculated with HF-srDFT orbitals and orbital energies. The MP2-srDFT approximation is obtained by truncating the perturbation expansion through second order, thus leading to the following energy expression

$$\begin{aligned} E_{\text{MP2}}^{\text{srDFT}} &= \langle \Phi_0^\mu | \hat{T} + \hat{V}_{\text{ne}} | \Phi_0^\mu \rangle + E_{\text{H}}[n_{\Phi_0^\mu}] + E_{\text{x}}^{\text{HF}}[\Phi_0^\mu] - E_{\text{x}}^{\text{HF,sr},\mu}[\Phi_0^\mu] \\ &\quad + E_{\text{x}}^{\text{sr},\mu}[n_{\Phi_0^\mu}] + E_{\text{MP}}^{(2)\text{lr},\mu} + E_{\text{c}}^{\text{sr},\mu}[n_{\Phi_0^\mu}], \end{aligned} \quad (24)$$

where $E_{\text{x}}^{\text{HF}}[\Phi_0^\mu]$ and $E_{\text{x}}^{\text{HF,sr},\mu}[\Phi_0^\mu]$ are the regular (full-range) and short-range HF exchange energies, respectively, both obtained from the HF-srDFT determinant. Eq. (24) defines a RSDH approximation where the exchange and correlation energies are

$$E_{\text{x,MP2}}^{\text{srDFT}} = E_{\text{x}}^{\text{HF}}[\Phi] - E_{\text{x}}^{\text{HF,sr},\mu}[\Phi] + E_{\text{x}}^{\text{sr},\mu}[n], \quad (25)$$

and

$$E_{\text{c,MP2}}^{\text{srDFT}} = E_{\text{MP}}^{(2)\text{lr},\mu} + E_{\text{c}}^{\text{sr},\mu}[n], \quad (26)$$

Φ and n being shorthand notations for the HF-srDFT determinant and its density, respectively.

Finally, as shown by Cornaton *et al.*⁷, combining the wavefunction expansion in Eq. (20) with the alternative energy expression in Eq. (16) leads to another type of RSDH approximation that involves, in the computation of the energy through first order, *full-range* integrals only. For that reason, the method was referred to as RSDHf in Ref.⁷ When second-order corrections to the density are neglected, the energy equals through second order⁷

$$\begin{aligned} E_{\text{RSDHf}} &= \langle \Phi_0^\mu | \hat{T} + \hat{V}_{\text{ne}} | \Phi_0^\mu \rangle + E_{\text{H}}[n_{\Phi_0^\mu}] + E_{\text{x}}^{\text{HF}}[\Phi_0^\mu] \\ &\quad + E_{\text{MP}}^{(2)\text{lr},\mu} + E_{\text{MP}}^{(2)\text{lr-sr},\mu} + E_{\text{c,md}}^{\text{sr},\mu}[n_{\Phi_0^\mu}], \end{aligned} \quad (27)$$

where $E_{\text{MP}}^{(2)\text{lr-sr},\mu}$ denotes the MP2 coupling term between long-range and short-range correlations calculated with HF-srDFT orbitals and orbital energies. The corresponding exchange and correlation energies are

$$E_{\text{x,RSDHf}} = E_{\text{x}}^{\text{HF}}[\Phi], \quad (28)$$

and

$$E_{\text{c,RSDHf}} = E_{\text{MP}}^{(2)\text{lr},\mu} + E_{\text{MP}}^{(2)\text{lr-sr},\mu} + E_{\text{c,md}}^{\text{sr},\mu}[n], \quad (29)$$

respectively, where the same shorthand notations as in Eqs. (25) and (26) are used.

2.2 Multi-determinant DFT based on the Coulomb-attenuating method

2.2.1 Coulomb-attenuating hybrid DFT

The partitioning of the universal LL functional underlying standard hybrid CAM-DFT (whose most popular approximate formulation is CAM-B3LYP¹¹) is obtained from Eq. (3) by substituting the α, β -dependent attenuated interaction for the purely long-range one,

$$w_{\text{ee}}^{\text{lr},\mu}(r_{12}) \rightarrow \alpha w_{\text{ee}}(r_{12}) + \beta w_{\text{ee}}^{\text{lr},\mu}(r_{12}), \quad (30)$$

with the relations $0 \leq \alpha + \beta \leq 1$, $0 \leq \alpha \leq 1$ and $0 \leq \beta \leq 1$, thus leading to

$$\begin{aligned} F[n] = & \left(\min_{\Phi \rightarrow n} \langle \Phi | \hat{T} + \alpha \hat{W}_{\text{ee}} + \beta \hat{W}_{\text{ee}}^{\text{lr},\mu} | \Phi \rangle \right) + (1 - \alpha - \beta) E_{\text{H}}[n] + \beta E_{\text{H}}^{\text{sr},\mu}[n] \\ & + (1 - \alpha - \beta) E_{\text{x}}[n] + \beta E_{\text{x}}^{\text{sr},\mu}[n] + U_{\text{c}}^{\mu,\alpha,\beta}[n]. \end{aligned} \quad (31)$$

According to the KS decomposition in Eq. (4), the *exact* complement correlation functional can be expressed as

$$\begin{aligned} U_{\text{c}}^{\mu,\alpha,\beta}[n] = & E_{\text{c}}[n] + \langle \Phi^{\text{KS}}[n] | \hat{T} + \alpha \hat{W}_{\text{ee}} + \beta \hat{W}_{\text{ee}}^{\text{lr},\mu} | \Phi^{\text{KS}}[n] \rangle \\ & - \left(\min_{\Phi \rightarrow n} \langle \Phi | \hat{T} + \alpha \hat{W}_{\text{ee}} + \beta \hat{W}_{\text{ee}}^{\text{lr},\mu} | \Phi \rangle \right). \end{aligned} \quad (32)$$

Combining Eq. (1) with Eq. (31) leads to the exact hybrid CAM-DFT energy expression

$$E = \min_{\Phi} \left\{ \langle \Phi | \hat{T} + \hat{V}_{\text{ne}} + \alpha \hat{W}_{\text{ee}} + \beta \hat{W}_{\text{ee}}^{\text{lr},\mu} | \Phi \rangle + (1 - \alpha - \beta) E_{\text{H}}[n_{\Phi}] + \beta E_{\text{H}}^{\text{sr},\mu}[n_{\Phi}] \right. \\ \left. + (1 - \alpha - \beta) E_{\text{x}}[n_{\Phi}] + \beta E_{\text{x}}^{\text{sr},\mu}[n_{\Phi}] + U_{\text{c}}^{\mu,\alpha,\beta}[n_{\Phi}] \right\}. \quad (33)$$

Note that, in practical calculations, the standard correlation functional $E_{\text{c}}[n]$ is used for $U_{\text{c}}^{\mu,\alpha,\beta}[n]$ ¹¹. Thus it is assumed that the last two terms on the right-hand side of Eq. (32) compensate. Let us stress that, in hybrid CAM-DFT, the CAM is used for the exchange energy only. The correlation energy is, like in hybrid LC-DFT or KS-DFT, described by a density functional. Consequently one single determinant is sufficient for computing the ground-state energy. The latter becomes *exact* when both exact short-range and regular (full-range) exchange energy density functionals are used in conjunction with the exact complement correlation functional.

2.2.2 Multi-determinantal extensions

We discuss in this section the multi-determinantal extension of hybrid CAM-DFT. In the light of Sec. 2.1.2, the most natural way to proceed consists in extending the minimization in the first term on the right-hand side of Eq. (31) to multi-determinantal wavefunctions with density n . A complement correlation functional, depending on both μ , α and β , should then be constructed so that the universal LL functional is recovered from the new partitioning. The resulting exact expression for the ground-state energy would then be formally identical to the range-separated one in Eq. (13). The only difference would come from the substitution in Eq. (30). Applying MP2 in this context would provide a CAM-DH energy expression. Let us stress that such a CAM-DH is not expected to converge as fast as MP2-srDFT and RSDHf with respect to the basis set⁷ simply because, unlike the purely long-range interaction, the Coulomb-attenuated interaction has a singularity at $r_{12} = 0$. Of course, using the CAM makes the electronic cusp condition weaker, since at short range the regular interaction $1/r_{12}$ is scaled by α , but still the singularity remains. In connection to this, basis set superposition errors (BSSE) are also expected to be larger relative to MP2-srDFT and RSDHf.

We choose here not to explore further such a CAM-DH scheme. We rather propose to keep the purely long-range MP2 wavefunction expansion underlying both MP2-srDFT and RSDHf while introducing Coulomb attenuation into the energy expression. This can be achieved rigorously by using the following decomposition of the srHxc density-functional energy,

$$E_{\text{Hxc}}^{\text{sr},\mu}[n] = \langle \Psi^\mu[n] | (\beta - 1) \hat{W}_{\text{ee}}^{\text{lr},\mu} + \alpha \hat{W}_{\text{ee}} | \Psi^\mu[n] \rangle + \bar{E}_{\text{Hxc}}^{\mu,\alpha,\beta}[n], \quad (34)$$

where the complement three-parameter density functional $\bar{E}_{\text{Hxc}}^{\mu,\alpha,\beta}[n]$ is such that the exact (μ -dependent only) srHxc energy is obtained for any values of α and β . Since⁷ $\Psi^\mu[n_{\Psi^\mu}] = \Psi^\mu$, the exact ground-state energy expression in Eq. (13) becomes with the partitioning in Eq. (34),

$$E = \langle \Psi^\mu | \hat{T} + \hat{V}_{\text{ne}} + \beta \hat{W}_{\text{ee}}^{\text{lr},\mu} + \alpha \hat{W}_{\text{ee}} | \Psi^\mu \rangle + \bar{E}_{\text{Hxc}}^{\mu,\alpha,\beta}[n_{\Psi^\mu}], \quad (35)$$

thus leading to a multi-determinantal extension of hybrid CAM-DFT. Note that, for $\alpha = 0, \beta = 1$ and $\alpha = 1, \beta = 0$, the energy expressions underlying MP2-srDFT and RSDHf methods are recovered, respectively.

It is essential, in order to perform practical calculations along those lines, to provide a more explicit expression for the complement functional $\bar{E}_{\text{Hxc}}^{\mu,\alpha,\beta}[n]$ so that density functional approximations (DFAs) can be developed. For that purpose, we rewrite Eq. (34) as

$$\bar{E}_{\text{Hxc}}^{\mu,\alpha,\beta}[n] = E_{\text{Hxc}}^{\text{sr},\mu}[n] - \alpha \langle \Psi^\mu[n] | \hat{W}_{\text{ee}}^{\text{sr},\mu} | \Psi^\mu[n] \rangle + (1 - \alpha - \beta) \langle \Psi^\mu[n] | \hat{W}_{\text{ee}}^{\text{lr},\mu} | \Psi^\mu[n] \rangle, \quad (36)$$

thus leading to, according to Eq. (14),

$$\bar{E}_{\text{Hxc}}^{\mu,\alpha,\beta}[n] = (1 - \alpha) E_{\text{Hxc}}^{\text{sr},\mu}[n] + \alpha E_{\text{c,md}}^{\text{sr},\mu}[n] + (1 - \alpha - \beta) \langle \Psi^\mu[n] | \hat{W}_{\text{ee}}^{\text{lr},\mu} | \Psi^\mu[n] \rangle. \quad (37)$$

As mentioned previously, local DFAs^{18,19} have been developed for the first two contributions on the right-hand side of Eq. (37). On the other hand, the last term needs to be further simplified. As shown in Sec. 2.3, the latter can be expressed in terms of conventional and short-range exchange–correlation functionals by means of a double adiabatic connection and the use of scaling relations.

2.3 Double adiabatic connection

We use in this section a double adiabatic connection (AC) where the two-electron interaction strength depends not only on the range-separation parameter μ (like in range-dependent ACs^{25–28}) but also on a scaling factor λ (like in regular linear ACs^{4–6,29}). This leads to the following auxiliary equations

$$\left(\hat{T} + \lambda\hat{W}_{\text{ee}}^{\text{lr},\mu} + \hat{V}^{\mu,\lambda}\right)|\Psi^{\mu,\lambda}\rangle = \mathcal{E}^{\mu,\lambda}|\Psi^{\mu,\lambda}\rangle, \quad (38)$$

where the local potential operator $\hat{V}^{\mu,\lambda} = \int d\mathbf{r} v^{\mu,\lambda}(\mathbf{r}) \hat{n}(\mathbf{r})$ ensures that the density constraint

$$n_{\Psi^{\mu,\lambda}}(\mathbf{r}) = n(\mathbf{r}) \quad (39)$$

is fulfilled for all λ and μ values. Note that such an AC can in principle be described accurately by using Legendre–Fenchel transforms in conjunction with an expansion of the local potential in a given (finite) basis set and the computation of the partially-interacting wavefunction at the Coupled-Cluster level^{27–30}.

Let us consider the partially long-range-interacting LL functional

$$F^{\text{lr},\mu,\lambda}[n] = \min_{\Psi \rightarrow n} \langle \Psi | \hat{T} + \lambda\hat{W}_{\text{ee}}^{\text{lr},\mu} | \Psi \rangle = \langle \Psi^{\mu,\lambda} | \hat{T} + \lambda\hat{W}_{\text{ee}}^{\text{lr},\mu} | \Psi^{\mu,\lambda} \rangle, \quad (40)$$

and its KS decomposition

$$F^{\text{lr},\mu,\lambda}[n] = T_{\text{s}}[n] + E_{\text{Hxc}}^{\text{lr},\mu,\lambda}[n]. \quad (41)$$

Using $T_{\text{s}}[n] = F^{\text{lr},\mu,0}[n]$, the partially long-range interacting Hxc energy can be expressed as

$$E_{\text{Hxc}}^{\text{lr},\mu,\lambda}[n] = \int_0^\lambda d\nu \frac{dF^{\text{lr},\mu,\nu}[n]}{d\nu}, \quad (42)$$

thus leading to, according to the Hellmann–Feynman theorem and the density constraint in Eq. (39),

$$E_{\text{Hxc}}^{\text{lr},\mu,\lambda}[n] = \int_0^\lambda d\nu \langle \Psi^{\mu,\nu} | \hat{W}_{\text{ee}}^{\text{lr},\mu} | \Psi^{\mu,\nu} \rangle, \quad (43)$$

or, equivalently,

$$\frac{\partial E_{\text{Hxc}}^{\text{lr},\mu,\lambda}[n]}{\partial \lambda} = \langle \Psi^{\mu,\lambda} | \hat{W}_{\text{ee}}^{\text{lr},\mu} | \Psi^{\mu,\lambda} \rangle. \quad (44)$$

Following Toulouse *et al.*³¹ and Yang²⁵, we express the density-functional energy in Eq. (43) as

$$\begin{aligned} E_{\text{Hxc}}^{\text{lr},\mu,\lambda}[n] &= \lambda(E_{\text{H}}[n] - E_{\text{H}}^{\text{sr},\mu}[n]) + \lambda(E_{\text{x}}[n] - E_{\text{x}}^{\text{sr},\mu}[n]) \\ &\quad + \lambda^2(E_{\text{c}}[n_{1/\lambda}] - E_{\text{c}}^{\text{sr},\mu/\lambda}[n_{1/\lambda}]), \end{aligned} \quad (45)$$

where the scaled density $n_{1/\lambda}$ is defined as follows

$$n_{1/\lambda}(\mathbf{r}) = (1/\lambda)^3 n(\mathbf{r}/\lambda). \quad (46)$$

In the particular case where $\lambda = 1$, $\Psi^{\mu,\lambda}$ reduces to the long-range-interacting wavefunction $\Psi^{\mu}[n]$ introduced in Eq. (8). We therefore obtain from Eq. (44),

$$\begin{aligned} \langle \Psi^{\mu}[n] | \hat{W}_{\text{ee}}^{\text{lr},\mu} | \Psi^{\mu}[n] \rangle &= \left. \frac{\partial E_{\text{Hxc}}^{\text{lr},\mu,\lambda}[n]}{\partial \lambda} \right|_{\lambda=1} \\ &= (E_{\text{H}}[n] - E_{\text{H}}^{\text{sr},\mu}[n]) + (E_{\text{x}}[n] - E_{\text{x}}^{\text{sr},\mu}[n]) \\ &\quad + 2(E_{\text{c}}[n] - E_{\text{c}}^{\text{sr},\mu}[n]) \\ &\quad + \left. \frac{\partial}{\partial \lambda} (E_{\text{c}}[n_{1/\lambda}] - E_{\text{c}}^{\text{sr},\mu/\lambda}[n_{1/\lambda}]) \right|_{\lambda=1}, \end{aligned} \quad (47)$$

thus leading to the exact expression for the complement density-functional energy in Eq. (37):

$$\begin{aligned} \bar{E}_{\text{Hxc}}^{\mu,\alpha,\beta}[n] &= (1 - \alpha - \beta)E_{\text{H}}[n] + \beta E_{\text{H}}^{\text{sr},\mu}[n] \\ &\quad + (1 - \alpha - \beta)E_{\text{x}}[n] + \beta E_{\text{x}}^{\text{sr},\mu}[n] \\ &\quad + 2(1 - \alpha - \beta)E_{\text{c}}[n] - (1 - \alpha - 2\beta)E_{\text{c}}^{\text{sr},\mu}[n] + \alpha E_{\text{c,md}}^{\text{sr},\mu}[n] \\ &\quad + (1 - \alpha - \beta) \left. \frac{\partial}{\partial \lambda} (E_{\text{c}}[n_{1/\lambda}] - E_{\text{c}}^{\text{sr},\mu/\lambda}[n_{1/\lambda}]) \right|_{\lambda=1}. \end{aligned} \quad (48)$$

As suggested by Sharkas *et al.*⁴ for double hybrids based on the linear separation of the two-electron interaction, density scaling might be neglected in practical calculations,

$$E_{\text{c}}[n_{1/\lambda}] \rightarrow E_{\text{c}}[n], \quad E_{\text{c}}^{\text{sr},\mu/\lambda}[n_{1/\lambda}] \rightarrow E_{\text{c}}^{\text{sr},\mu/\lambda}[n], \quad (49)$$

which leads to the following approximate expression

$$\begin{aligned}
\bar{E}_{\text{Hxc}}^{\mu,\alpha,\beta}[n] \rightarrow & (1 - \alpha - \beta)E_{\text{H}}[n] + \beta E_{\text{H}}^{\text{sr},\mu}[n] \\
& + (1 - \alpha - \beta)E_{\text{x}}[n] + \beta E_{\text{x}}^{\text{sr},\mu}[n] \\
& + 2(1 - \alpha - \beta)E_{\text{c}}[n] - (1 - \alpha - 2\beta)E_{\text{c}}^{\text{sr},\mu}[n] + \alpha E_{\text{c,md}}^{\text{sr},\mu}[n] \\
& + \mu(1 - \alpha - \beta) \frac{\partial E_{\text{c}}^{\text{sr},\mu}[n]}{\partial \mu}.
\end{aligned} \tag{50}$$

2.4 Coulomb-attenuating double hybrid approximation

In order to derive a CAM-DH scheme from the exact energy expression in Eq. (35), we now introduce the modified auxiliary energy

$$E^{\epsilon,\mu,\alpha,\beta} = E^{\epsilon,\mu} - E_{\text{Hxc}}^{\text{sr},\mu}[n_{\Psi^{\epsilon,\mu}}] + \epsilon \frac{\langle \Psi^{\epsilon,\mu} | \alpha \hat{W}_{\text{ee}} + (\beta - 1) \hat{W}_{\text{ee}}^{\text{lr},\mu} | \Psi^{\epsilon,\mu} \rangle}{\langle \Psi^{\epsilon,\mu} | \Psi^{\epsilon,\mu} \rangle} + \bar{E}_{\text{Hxc}}^{\mu,\alpha,\beta}[n_{\Psi^{\epsilon,\mu}}], \tag{51}$$

where $E^{\epsilon,\mu}$ is the original auxiliary energy underlying the MP2-srDFT method (See Eq. (19)). Note that both original and modified auxiliary energies are equal to the *exact* ground-state energy when $\epsilon = 1$. Following Ref.⁷ leads to the second-order expansion

$$E^{\epsilon,\mu,\alpha,\beta} = E^{(0)\mu,\alpha,\beta} + \epsilon E^{(1)\mu,\alpha,\beta} + \epsilon^2 E^{(2)\mu,\alpha,\beta} + \mathcal{O}(\epsilon^3), \tag{52}$$

where the energy recovered through first order equals

$$E^{(0)\mu,\alpha,\beta} + E^{(1)\mu,\alpha,\beta} = \langle \Phi_0^\mu | \hat{T} + \alpha \hat{W}_{\text{ee}} + \beta \hat{W}_{\text{ee}}^{\text{lr},\mu} + \hat{V}_{\text{ne}} | \Phi_0^\mu \rangle + \bar{E}_{\text{Hxc}}^{\mu,\alpha,\beta}[n_{\Phi_0^\mu}], \tag{53}$$

and the second-order energy correction is

$$\begin{aligned}
E^{(2)\mu,\alpha,\beta} = & (2(\alpha + \beta) - 1) E_{\text{MP}}^{(2)\text{lr},\mu} + \alpha E_{\text{MP}}^{(2)\text{lr-sr},\mu} \\
& + \int d\mathbf{r} \left(\frac{\delta \bar{E}_{\text{Hxc}}^{\mu,\alpha,\beta}}{\delta n(\mathbf{r})} - \frac{\delta E_{\text{Hxc}}^{\text{sr},\mu}}{\delta n(\mathbf{r})} \right) [n_{\Phi_0^\mu}] \delta n^{(2)\mu}(\mathbf{r}).
\end{aligned} \tag{54}$$

When the second-order correction to the density as well as density scaling in the complement density-functional energy are neglected, a CAM-DH energy expression referred to as d μ -

CAM-DH lr is obtained

$$\begin{aligned}
E_{\text{d}\mu\text{-CAM}}^{\text{DH}lr} &= \langle \Phi_0^\mu | \hat{T} + \hat{V}_{\text{ne}} | \Phi_0^\mu \rangle + E_{\text{H}}[n_{\Phi_0^\mu}] + (\alpha + \beta) E_{\text{x}}^{\text{HF}}[\Phi_0^\mu] - \beta E_{\text{x}}^{\text{HF},\text{sr},\mu}[\Phi_0^\mu] \\
&+ (1 - \alpha - \beta) E_{\text{x}}[n_{\Phi_0^\mu}] + \beta E_{\text{x}}^{\text{sr},\mu}[n_{\Phi_0^\mu}] \\
&+ (2(\alpha + \beta) - 1) E_{\text{MP}}^{(2)\text{lr},\mu} + \alpha E_{\text{MP}}^{(2)\text{lr-sr},\mu} \\
&+ 2(1 - \alpha - \beta) E_{\text{c}}[n_{\Phi_0^\mu}] - (1 - \alpha - 2\beta) E_{\text{c}}^{\text{sr},\mu}[n_{\Phi_0^\mu}] + \alpha E_{\text{c,md}}^{\text{sr},\mu}[n_{\Phi_0^\mu}] \\
&+ \mu(1 - \alpha - \beta) \left. \frac{\partial E_{\text{c}}^{\text{sr},\nu}[n_{\Phi_0^\mu}]}{\partial \nu} \right|_{\nu=\mu}. \tag{55}
\end{aligned}$$

The corresponding expressions for the exchange and correlation energies are

$$\begin{aligned}
E_{\text{x,d}\mu\text{-CAM}}^{\text{DH}lr} &= (\alpha + \beta) E_{\text{x}}^{\text{HF}}[\Phi] - \beta E_{\text{x}}^{\text{HF},\text{sr},\mu}[\Phi] \\
&+ (1 - \alpha - \beta) E_{\text{x}}[n] + \beta E_{\text{x}}^{\text{sr},\mu}[n], \tag{56}
\end{aligned}$$

and

$$\begin{aligned}
E_{\text{c,d}\mu\text{-CAM}}^{\text{DH}lr} &= (2(\alpha + \beta) - 1) E_{\text{MP}}^{(2)\text{lr},\mu} + \alpha E_{\text{MP}}^{(2)\text{lr-sr},\mu} \\
&+ 2(1 - \alpha - \beta) E_{\text{c}}[n] - (1 - \alpha - 2\beta) E_{\text{c}}^{\text{sr},\mu}[n] + \alpha E_{\text{c,md}}^{\text{sr},\mu}[n] \\
&+ \mu(1 - \alpha - \beta) \frac{\partial E_{\text{c}}^{\text{sr},\mu}[n]}{\partial \mu}. \tag{57}
\end{aligned}$$

Note that the suffix lr in $\text{d}\mu\text{-CAM-DH}lr$ refers to the *long-range* interacting perturbation theory this specific CAM-DH approximation relies on. The prefix "d μ " comes from the derivative with respect to the range-separation parameter μ in the last term on the right-hand side of Eq. (57). By neglecting this derivative, that we call $\text{d}\mu$ correction in the following, we obtain what we shall simply refer to as CAM-DH lr correlation energy

$$\begin{aligned}
E_{\text{c,CAM}}^{\text{DH}lr} &= (2(\alpha + \beta) - 1) E_{\text{MP}}^{(2)\text{lr},\mu} + \alpha E_{\text{MP}}^{(2)\text{lr-sr},\mu} \\
&+ 2(1 - \alpha - \beta) E_{\text{c}}[n] - (1 - \alpha - 2\beta) E_{\text{c}}^{\text{sr},\mu}[n] + \alpha E_{\text{c,md}}^{\text{sr},\mu}[n], \tag{58}
\end{aligned}$$

while the CAM-DH lr exchange energy will be the same as for $\text{d}\mu\text{-CAM-DH}lr$ (see Eq. (56)).

Interestingly, CAM-DH lr reduces to MP2-srDFT and RSDHf when $\alpha = 0, \beta = 1$ and $\alpha = 1, \beta = 0$, respectively. Using the linearity in α and β of the CAM-DH lr correlation energy leads to the compact expression

$$E_{\text{c,CAM}}^{\text{DH}lr} = \alpha E_{\text{c,RSDHf}} + \beta E_{\text{c,MP2}}^{\text{srDFT}} + (1 - \alpha - \beta) \left(2E_{\text{c}}[n] - E_{\text{c}}^{\text{sr},\mu}[n] - E_{\text{MP}}^{(2)\text{lr},\mu} \right). \tag{59}$$

Note finally that, in the particular case where $\alpha + \beta = 1$, CAM-DH*lr* reduces to the *two-parameter* RSDHf (2RSDHf) scheme introduced in the Appendix A of Ref.⁷ The second parameter (referred to as λ in Ref.⁷) is here equal to α .

3 COMPUTATIONAL DETAILS

The $(d\mu)$ -CAM-DH*lr* exchange and correlation energies in Eqs. (56), (57) and (59) have been computed with a development version of the DALTON program package³². Spin-unpolarized LDA-type functionals^{18,19} have been used for modeling complement density-functional energy contributions. The corresponding double hybrid approximations will therefore be referred to with the suffix LDA: $(d\mu)$ -CAM-DH*lr*-LDA, MP2-srLDA, RSDHf-LDA and 2RSDHf-LDA. The range-separation parameter was set to the prescribed value $\mu = 0.4a_0^{-1}$ (see Ref.⁷). Augmented correlation-consistent polarized quadruple- ζ basis sets ("aug-cc-pVQZ") of Dunning and co-workers³³⁻³⁸ have been used. Interaction energies have been computed for the first three noble-gas homonuclear dimers (He_2 , Ne_2 and Ar_2) as well as for the first two homonuclear alkaline-earth-metal dimers (Be_2 and Mg_2). Since both CAM and range-separated double hybrid schemes considered in this work rely on a long-range-interacting only perturbation theory, BSSE is expected to be small⁷. Consequently, no BSSE correction was made. In addition, total energies have been computed around the equilibrium distance for H_2 , Li_2 , C_2 , N_2 and F_2 .

4 RESULTS AND DISCUSSION

4.1 Results for He_2 , Ne_2 and Ar_2

As mentioned in Sec. 2.4, in the particular case where $\alpha + \beta = 1$, CAM-DH*lr*-LDA reduces to the 2RSDHf-LDA scheme of Ref.⁷, where the second parameter equals $\lambda = \alpha = 1 - \beta$. The 2RSDHf-LDA energy is in fact the weighted average value of RSDHf-LDA and MP2-srLDA energies with weights λ and $(1 - \lambda)$, respectively. Therefore, the long-range correlation energy is entirely described within MP2. On the other hand, the coupling between long- and short-range correlations is decomposed into MP2 and density-functional contributions.

Obviously, when applied to weakly interacting systems, 2RSDHf-LDA can only improve MP2-srLDA and RSDHf-LDA interaction energies around the equilibrium distance where the long-range–short-range MP2 coupling term can be significant⁷. For $0 < \lambda < 1$, the 2RSDHf-LDA curve will be located between the MP2-srLDA and RSDHf-LDA ones. The latter are shown in Fig. 1. Consequently, the agreement with experiment strongly depends on the performance of the MP2-srLDA and RSDHf-LDA methods. For He₂ and Ne₂, they both underestimate the interaction energy. In this particular case, 2RSDHf-LDA will bring no improvement relative to MP2-srLDA and RSDHf-LDA. In Ar₂, RSDHf-LDA overbinds while MP2-srLDA slightly underbinds. It is then possible to find a λ value for which the 2RSDHf-LDA interaction energy equals the experimental one. However, the equilibrium bond distance will then be overestimated and the interaction energy at long distance will remain overestimated (in absolute value). According to Ref.³⁹, substituting a long-range *Random-Phase Approximation* (RPA) for the long-range MP2 treatment may improve the potential curve at large distance. A more pragmatic alternative, that we investigate further in the following, consists in treating only a fraction of the long-range correlation energy within MP2.

We will therefore relax the condition $\alpha + \beta = 1$, in analogy with the hybrid CAM-B3LYP functional¹¹ where the Coulomb attenuation is used for the exchange energy only. Even though we are using the former for both exchange and correlation energies, it is interesting for analysis purposes to use the same parameters as in CAM-B3LYP ($\alpha = 0.19$ and $\beta = 0.46$). Unlike the value $\mu = 0.4$ that is based on the analysis of long-range correlation effects⁷, these two values have been optimized empirically in a completely different context. In this respect, the corresponding CAM-DH*lr*-LDA approach is semi-empirical. In contrast to 2RSDHf-LDA, the CAM-DH*lr*-LDA energy includes then a third term, in addition to the total RSDHf-LDA and MP2-srLDA energies. Indeed, according to Eqs. (56) and (59), the former can be rewritten as

$$\begin{aligned}
E_{\text{CAM}}^{\text{DH}lr\text{-LDA}} &= (1 - \alpha - \beta)(E_{\text{LDA}}^0 + E_c^{\text{LDA}}[n] - E_c^{\text{srLDA},\mu}[n] - E_{\text{MP}}^{(2)lr,\mu}) \\
&\quad + \alpha E_{\text{RSDHf}}^{\text{LDA}} + \beta E_{\text{MP2}}^{\text{srLDA}},
\end{aligned}
\tag{60}$$

where n denotes here the HF-srLDA density and E_{LDA}^0 is the conventional KS-LDA total

energy computed with the HF-srLDA determinant. Let us stress that, in this case, only a fraction $2(\alpha + \beta) - 1 = 0.3$ of the long-range correlation energy is described by MP2.

Each contribution to the first term on the right-hand side of Eq. (60) as well as the total CAM-DH lr -LDA interaction energy have been computed for the three dimers. Results are shown in Fig. 1. As expected⁴⁰, the total LDA energy contribution E_{LDA}^0 is always too attractive. For He₂ and Ne₂, the remaining contributions do not compensate this large error, which explains why CAM-DH lr -LDA strongly overbinds. On the other hand, for Ar₂, the overbinding induced by the total LDA energy contribution is less pronounced so that the significant long-range MP2 term compensates the error and leads to a CAM-DH lr -LDA curve that is significantly less attractive relative to MP2-srLDA and RSDHf-LDA. Note also that the potential curves are less accurate at long distance relative to MP2-srLDA, RSDHf-LDA and 2RSDHf-LDA.

These observations suggest that the parameters $\alpha = 0.19$ and $\beta = 0.46$ optimized for the CAM-B3LYP functional are not optimal in this context. As shown in Fig. 2, it is possible to tune α and β in order to obtain more accurate potential energy curves. Choosing $\alpha + \beta$ slightly smaller than 1 (between 0.8 and 0.9) seems to give the best results. Note that, in that case, CAM-DH lr -LDA performs much better than MP2-srLDA and RSDHf-LDA for Ar₂ at long distance. As discussed further in Sec. 5, it would also be interesting to test another formulation of CAM-DH where the perturbation expansion of the wavefunction is based on a partially long-range interacting system. In such an approach, the CAM-DH energy is not linear in α and β anymore.

Let us finally discuss the performance of the $d\mu$ -CAM-DH lr -LDA method that simply consists in adding to the CAM-DH lr -LDA energy the fraction $\mu(1 - \alpha - \beta)$ of the first-order derivative $\partial E_c^{\text{srLDA},\mu}[n]/\partial\mu$ at $\mu = 0.4a_0^{-1}$. Fig. 3 shows the variation with μ of the srLDA correlation interaction energy computed with the HF-srLDA ($\mu = 0.4$) density for different bond distances in He₂. That contribution is clearly linear in the vicinity of $0.4a_0^{-1}$. It is therefore relevant to approximate the first-order derivative as follows

$$\left. \frac{\partial E_c^{\text{srLDA},\mu}[n]}{\partial\mu} \right|_{\mu=0.4a_0^{-1}} \approx \frac{E_c^{\text{srLDA},\mu=0.405a_0^{-1}}[n] - E_c^{\text{srLDA},\mu=0.395a_0^{-1}}[n]}{0.01}. \quad (61)$$

Fig 3. in Ref.⁷ suggests that this approximation is also relevant for the other dimers. Results

obtained for the semi-empirical $\alpha = 0.19$ and $\beta = 0.46$ parameters are shown in Fig. 4. As expected from Fig. 3 (where the slope of the srLDA correlation interaction energy is always positive), $d\mu$ -CAM-DH*lr*-LDA binds less than CAM-DH*lr*-LDA. The difference is quite significant which is an improvement for He₂ and Ne₂ but not for Ar₂.

4.2 Results for Be₂ and Mg₂

Interaction energies have been computed for the first two alkaline-earth-metal dimers. The beryllium dimer is difficult to describe with DFT-based methods because (i) dispersion forces bind the two atoms and (ii) the latter exhibit significant multiconfigurational effects due to the low-lying 2p orbitals⁴¹. A multireference extension⁴² of CAM-DH*lr* would actually be more appropriate in this context. This is left for future work.

Here we discuss the interaction energy curves obtained at the CAM-DH*lr*-LDA level. Results are shown in Fig. 5 and comparison is made with MP2-srLDA and RSDHf-LDA. We first note that, in contrast to the rare-gas dimers, both Be₂ and Mg₂ have equilibrium interaction energies that are larger in absolute value at the MP2-srLDA level, relative to RSDHf-LDA. Both methods underbind while CAM-DH*lr*-LDA, using the semi-empirical $\alpha = 0.19$ and $\beta = 0.46$ parameters, overbinds. In the latter case, the energy contribution that is recovered when $\alpha = 0, \beta = 0$ (first term on the right-hand side of Eq. (60)) is too attractive and the scaling factor $1 - 0.19 - 0.46 = 0.35$ is large enough to induce overbinding. Like in the rare-gas dimers, using $\alpha = 0.2, \beta = 0.7$ or $\alpha = 0.6, \beta = 0.3$ provides reasonable equilibrium interaction energies. On the other hand, no improvement is observed at long distance.

Finally, the $d\mu$ correction has been computed when $\alpha = 0.19$ and $\beta = 0.46$. As observed for the rare-gas dimers, it reduces the equilibrium interaction energy which is an improvement for Be₂ but not for Mg₂. The performance of the $d\mu$ -CAM-DH*lr*-LDA scheme obviously depends on the choice of α and β . Density scaling in the correlation functionals is also expected to be important^{4,43}. Enlarging the test set and fitting all parameters on experimental data would be necessary at this point.

4.3 Results for H₂, Li₂, C₂, N₂ and F₂

We now consider diatomics with single σ bond (H₂, Li₂ and F₂), triple $\sigma + \pi + \pi$ bond (N₂) and even the unusual double $\pi + \pi$ bond (C₂). Note that, in order to describe the dissociation regime, a multiconfiguration hybrid CAM-DFT approach should be developed, in the spirit of multiconfiguration DFT based on the linear⁴⁴ and range^{45–47} separations of the two-electron repulsion. We focus here on the total energies around the equilibrium distances. Potential energy curves are shown in Fig. 6. While MP2-srLDA underestimates the total energies in absolute value, RSDHf-LDA energies are too low. CAM-DH lr -LDA is slightly more accurate than MP2-srLDA when the semi-empirical $\alpha = 0.19$ and $\beta = 0.46$ parameters are used. Note that the $d\mu$ correction to the total energy is positive, thus leading to a $d\mu$ -CAM-DH lr -LDA energy that is higher than the CAM-DH lr -LDA one and therefore less accurate for these systems. Let us mention that Toulouse *et al.* already observed in the helium atom that the srLDA correlation energy has a positive slope at $\mu = 0.4$ (see Fig. 6 in Ref.⁴⁸). Note that CAM-DH lr -LDA total energies obtained with the parameters $\alpha = 0.6, \beta = 0.3$ (see Sec. 4.1) are in relatively good agreement with the accurate values.

5 PERSPECTIVE: ALTERNATIVE FORMULATION OF THE CAM-DH APPROXIMATION

All the double hybrid energy expressions derived and tested previously rely on the perturbation expansion of a fully long-range interacting wavefunction. This choice was motivated by the fact that the long-range interaction based on the error function has no singularity at $r_{12} = 0$. Consequently, the BSSE is significantly reduced and the convergence with respect to the atomic basis set is faster relative to regular MP2 (see Ref.⁷ and the references therein). Such features would actually be preserved if a partially long-range interacting wavefunction was used instead. This choice seems in fact more sound since, within a CAM-DH scheme, we aim at describing only a fraction ($\alpha + \beta$) of the long-range interaction within MP2.

In order to derive such an alternative CAM-DH, we first consider the following decom-

position of the universal LL functional,

$$\begin{aligned} F[n] &= F^{\text{lr},+\infty,1}[n] \\ &= F^{\text{lr},+\infty,\lambda}[n] + (1 - \lambda)(E_{\text{H}}[n] + E_{\text{x}}[n]) + E_{\text{c}}[n] - \lambda^2 E_{\text{c}}[n_{1/\lambda}]. \end{aligned} \quad (62)$$

The latter relies on the linear separation of the two-electron repulsion⁶. We then separate the partially-interacting LL functional into long- and short-range parts

$$F^{\text{lr},+\infty,\lambda}[n] = F^{\text{lr},\mu,\lambda}[n] + E_{\text{Hxc}}^{\text{sr},\mu,\lambda}[n], \quad (63)$$

where, according to Refs.^{25,31},

$$E_{\text{Hxc}}^{\text{sr},\mu,\lambda}[n] = \lambda(E_{\text{H}}^{\text{sr},\mu}[n] + E_{\text{x}}^{\text{sr},\mu}[n]) + \lambda^2 E_{\text{c}}^{\text{sr},\mu/\lambda}[n_{1/\lambda}]. \quad (64)$$

We finally obtain from Eq. (62) the following decomposition for the LL functional

$$F[n] = F^{\text{lr},\mu,\lambda}[n] + \bar{E}_{\text{Hxc}}^{\mu,\lambda}[n], \quad (65)$$

where the complement density-functional energy equals

$$\begin{aligned} \bar{E}_{\text{Hxc}}^{\mu,\lambda}[n] &= \lambda(E_{\text{H}}^{\text{sr},\mu}[n] + E_{\text{x}}^{\text{sr},\mu}[n]) + (1 - \lambda)(E_{\text{H}}[n] + E_{\text{x}}[n]) \\ &\quad + \lambda^2 E_{\text{c}}^{\text{sr},\mu/\lambda}[n_{1/\lambda}] + E_{\text{c}}[n] - \lambda^2 E_{\text{c}}[n_{1/\lambda}]. \end{aligned} \quad (66)$$

According to the variational principle in Eq. (1), the *exact* ground-state energy can then be rewritten as

$$\begin{aligned} E &= \min_{\Psi} \left\{ \langle \Psi | \hat{T} + \hat{V}_{\text{ne}} + \lambda \hat{W}_{\text{ee}}^{\text{lr},\mu} | \Psi \rangle + \bar{E}_{\text{Hxc}}^{\mu,\lambda}[n_{\Psi}] \right\} \\ &= \langle \tilde{\Psi}^{\mu,\lambda} | \hat{T} + \hat{V}_{\text{ne}} + \lambda \hat{W}_{\text{ee}}^{\text{lr},\mu} | \tilde{\Psi}^{\mu,\lambda} \rangle + \bar{E}_{\text{Hxc}}^{\mu,\lambda}[n_{\tilde{\Psi}^{\mu,\lambda}}], \end{aligned} \quad (67)$$

where the minimizing wavefunction $\tilde{\Psi}^{\mu,\lambda}$ is the ground state of the partially long-range interacting system whose density equals the *exact* ground-state density of the physical system. A new class of range-separated double hybrids can then be formulated when solving Eq. (67) with many-body perturbation theory techniques.

By analogy with the HF-srDFT approximation, we obtain a *two-parameter range-separated hybrid* (2RSH) determinant,

$$\Phi_0^{\mu,\lambda} = \arg \min_{\Phi} \left\{ \langle \Phi | \hat{T} + \lambda \hat{W}_{\text{ee}}^{\text{lr},\mu} + \hat{V}_{\text{ne}} | \Phi \rangle + \bar{E}_{\text{Hxc}}^{\mu,\lambda}[n_{\Phi}] \right\}, \quad (68)$$

when restricting the minimization in Eq. (67) to single determinants Φ . Using a MP-type perturbation theory^{1,3,23} in this context leads to the following perturbation expansion for the energy

$$E = \langle \Phi_0^{\mu,\lambda} | \hat{T} + \hat{V}_{\text{ne}} + \lambda \hat{W}_{\text{ee}}^{\text{lr},\mu} | \Phi_0^{\mu,\lambda} \rangle + \bar{E}_{\text{Hxc}}^{\mu,\lambda}[n_{\Phi_0^{\mu,\lambda}}] + \lambda^2 E_{\text{MP}}^{(2)\text{lr},\mu} + \dots \quad (69)$$

If, instead, we split the complement density functional into wavefunction and density-functional terms as follows

$$\bar{E}_{\text{Hxc}}^{\mu,\lambda}[n] = \alpha \langle \Psi^{\mu,\lambda}[n] | \hat{W}_{\text{ee}}^{\text{sr},\mu} | \Psi^{\mu,\lambda}[n] \rangle + \bar{E}_{\text{Hxc}}^{\mu,\lambda,\alpha}[n], \quad (70)$$

where, according to the Appendix,

$$\begin{aligned} \bar{E}_{\text{Hxc}}^{\mu,\lambda,\alpha}[n] &= (\lambda - \alpha)(E_{\text{H}}^{\text{sr},\mu}[n] + E_{\text{x}}^{\text{sr},\mu}[n]) + (1 - \lambda)(E_{\text{H}}[n] + E_{\text{x}}[n]) \\ &\quad + \lambda(\lambda - \alpha)E_{\text{c}}^{\text{sr},\mu/\lambda}[n_{1/\lambda}] + E_{\text{c}}[n] - \lambda^2 E_{\text{c}}[n_{1/\lambda}] \\ &\quad + \alpha \lambda E_{\text{c,md}}^{\text{sr},\mu/\lambda}[n_{1/\lambda}], \end{aligned} \quad (71)$$

the *exact* ground-state energy can be rewritten, according to Eq. (67), as

$$E = \langle \tilde{\Psi}^{\mu,\lambda} | \hat{T} + \hat{V}_{\text{ne}} + \lambda \hat{W}_{\text{ee}}^{\text{lr},\mu} + \alpha \hat{W}_{\text{ee}}^{\text{sr},\mu} | \tilde{\Psi}^{\mu,\lambda} \rangle + \bar{E}_{\text{Hxc}}^{\mu,\lambda,\alpha}[n_{\tilde{\Psi}^{\mu,\lambda}}], \quad (72)$$

since $\Psi^{\mu,\lambda}[n_{\tilde{\Psi}^{\mu,\lambda}}] = \tilde{\Psi}^{\mu,\lambda}$.

A MP2-type perturbation theory similar to the one derived in Sec. 2.4 can then be formulated, thus leading to the following perturbation expansion for the energy through second order

$$\begin{aligned} E &= \langle \Phi_0^{\mu,\lambda} | \hat{T} + \hat{V}_{\text{ne}} + \lambda \hat{W}_{\text{ee}}^{\text{lr},\mu} + \alpha \hat{W}_{\text{ee}}^{\text{sr},\mu} | \Phi_0^{\mu,\lambda} \rangle + \bar{E}_{\text{Hxc}}^{\mu,\lambda,\alpha}[n_{\Phi_0^{\mu,\lambda}}] \\ &\quad + \lambda^2 E_{\text{MP}}^{(2)\text{lr},\mu} + \alpha \lambda E_{\text{MP}}^{(2)\text{lr-sr},\mu} + \dots, \end{aligned} \quad (73)$$

where the second-order correction to the density has been neglected. Note that the long-range and long-range-short-range MP2 correlation energies are obtained from the 2RSH orbitals and orbital energies. Therefore, they depend implicitly on λ .

Thus, we obtain an alternative CAM-DH approximation which can be compared with the $d\mu$ -CAM-DH/*lr* energy expression in Eq. (55) when choosing $\lambda = \alpha + \beta$. Interestingly,

the fractions of long-range and long-range–short-range MP2 correlation energies are now quadratic in α and β . They are equal to $(\alpha + \beta)^2$ and $\alpha(\alpha + \beta)$, respectively. The implementation and calibration of this approach that we could refer to as CAM-DH plr , where plr refers to the *partially long-range* interacting perturbation theory it relies on, is left for future work.

6 CONCLUSIONS

The rigorous formulation of Coulomb-attenuating double-hybrid methods (CAM-DH) has been investigated. In order to preserve the advantages of existing range-separated double hybrids (relatively fast convergence with respect to the basis set, small BSSE), we opted for a CAM-DH that relies on the perturbation expansion of a long-range interacting wavefunction, in the spirit of Ref.⁷ The method has been tested within the local density approximation on a small test set consisting of rare-gas and alkaline-earth-metal dimers as well as diatomics with single, double and triple bonds. In this context, the semi-empirical $\alpha = 0.19$ and $\beta = 0.46$ CAM parameters, that were optimized for the hybrid CAM-B3LYP functional, do not provide accurate interaction and total energies. Better results are obtained when $\alpha + \beta$ is closer (but not equal) to 1, at least within the formulation we opted for. Calibration studies should be performed on a larger test set. The benzene dimer and charge-transfer complexes (*e.g.* HCN \cdots NH₃⁴⁹) would be good candidates. Work is in progress in this direction. Note that density scaling in the complement correlation functional has not been taken into account in this work, though the effect is expected to be important⁴. This as well as the construction of CAM-DH using semi-local complement functionals^{4,43} should obviously be investigated further in the future. All parameters could be fitted on experimental data but, in the light of Ref.⁶, it would also be interesting for rationalizing the fitted parameters to derive and compute the approximate double adiabatic connection underlying CAM-DH and compare with accurate *ab initio* calculations. An alternative formulation of CAM-DH has finally been discussed as a perspective. It relies on the perturbation expansion of a partially long-range interacting wavefunction. In contrast to the CAM-DH tested in this work, the correlation energy is not linear in α and β anymore. The implementation and calibration of

such an approach is left for future work.

ACKNOWLEDGMENTS

The authors would like to thank Yann Schaerer and Julien Toulouse for fruitful discussions. EF thanks ANR (DYQUMA project) and LabEx "Chimie des Systèmes Complexes" for funding.

APPENDIX: scaling relation for the multi-determinantal short-range exact exchange energy

By analogy with Eq. (14), we consider the following decomposition of the partial short-range density-functional energy

$$E_{\text{Hxc}}^{\text{sr},\mu,\lambda}[n] = \lambda \langle \Psi^{\mu,\lambda}[n] | \hat{W}_{\text{ee}}^{\text{sr},\mu} | \Psi^{\mu,\lambda}[n] \rangle + E_{\text{c,md}}^{\text{sr},\mu,\lambda}[n]. \quad (\text{A1})$$

Since, according to Ref. ³¹,

$$\Psi^{\mu\gamma}[n_\gamma] = \Psi_\gamma^{\mu,1/\gamma}[n], \quad (\text{A2})$$

where for any N -electron wavefunction Ψ ,

$$\Psi_\gamma(\mathbf{r}_1, \dots, \mathbf{r}_N) = \gamma^{3N/2} \Psi(\gamma \mathbf{r}_1, \dots, \gamma \mathbf{r}_N), \quad (\text{A3})$$

we obtain the following scaling relation

$$\langle \Psi^{\mu\gamma}[n_\gamma] | \hat{W}_{\text{ee}}^{\text{sr},\mu\gamma} | \Psi^{\mu\gamma}[n_\gamma] \rangle = \gamma \langle \Psi^{\mu,1/\gamma}[n] | \hat{W}_{\text{ee}}^{\text{sr},\mu} | \Psi^{\mu,1/\gamma}[n] \rangle, \quad (\text{A4})$$

which, according to Eq. (64) as well as Eqs. (17) and (18) in Ref. ³¹, leads to

$$\begin{aligned} \gamma^2 E_{\text{c,md}}^{\text{sr},\mu,1/\gamma}[n] &= \gamma^2 \left(E_{\text{Hxc}}^{\text{sr},\mu,1/\gamma}[n] - \frac{1}{\gamma} \langle \Psi^{\mu,1/\gamma}[n] | \hat{W}_{\text{ee}}^{\text{sr},\mu} | \Psi^{\mu,1/\gamma}[n] \rangle \right) \\ &= E_{\text{Hxc}}^{\text{sr},\mu\gamma}[n_\gamma] - \langle \Psi^{\mu\gamma}[n_\gamma] | \hat{W}_{\text{ee}}^{\text{sr},\mu\gamma} | \Psi^{\mu\gamma}[n_\gamma] \rangle \\ &= E_{\text{c,md}}^{\text{sr},\mu\gamma}[n_\gamma]. \end{aligned} \quad (\text{A5})$$

In the particular case where $\gamma = 1/\lambda$, we obtain from Eqs. (64) and (A1)

$$\begin{aligned}
\lambda \langle \Psi^{\mu,\lambda}[n] | \hat{W}_{ee}^{\text{sr},\mu} | \Psi^{\mu,\lambda}[n] \rangle &= E_{\text{Hxc}}^{\text{sr},\mu,\lambda}[n] - E_{\text{c,md}}^{\text{sr},\mu,\lambda}[n] \\
&= \lambda (E_{\text{H}}^{\text{sr},\mu}[n] + E_{\text{x}}^{\text{sr},\mu}[n]) + \lambda^2 E_{\text{c}}^{\text{sr},\mu/\lambda}[n_{1/\lambda}] \\
&\quad - \lambda^2 E_{\text{c,md}}^{\text{sr},\mu/\lambda}[n_{1/\lambda}],
\end{aligned} \tag{A6}$$

or, equivalently,

$$\langle \Psi^{\mu,\lambda}[n] | \hat{W}_{ee}^{\text{sr},\mu} | \Psi^{\mu,\lambda}[n] \rangle = E_{\text{H}}^{\text{sr},\mu}[n] + E_{\text{x}}^{\text{sr},\mu}[n] + \lambda E_{\text{c}}^{\text{sr},\mu/\lambda}[n_{1/\lambda}] - \lambda E_{\text{c,md}}^{\text{sr},\mu/\lambda}[n_{1/\lambda}]. \tag{A7}$$

Combining Eq. (A7) with Eqs. (66) and (70) leads to Eq. (71).

References

1. J. G. Ángyán, I. C. Gerber, A. Savin, and J. Toulouse, *Phys. Rev. A* **72**, 012510 (2005).
2. E. Goll, H. J. Werner, and H. Stoll, *Phys. Chem. Chem. Phys.* **7**, 3917 (2005).
3. E. Fromager and H. J. Aa. Jensen, *Phys. Rev. A* **78**, 022504 (2008).
4. K. Sharkas, J. Toulouse, and A. Savin, *J. Chem. Phys.* **134**, 064113 (2011).
5. E. Fromager, *J. Chem. Phys.* **135**, 244106 (2011).
6. Y. Cornaton, O. Franck, A. M. Teale, and E. Fromager, *Mol. Phys.* **111**, 1275 (2013).
7. Y. Cornaton, A. Stoyanova, H. J. Aa. Jensen, and E. Fromager, *Phys. Rev. A* **88**, 022516 (2013).
8. A. Savin, *Recent Developments and Applications of Modern Density Functional Theory* (Elsevier, Amsterdam, 1996), p. 327.
9. A. D. Becke, *J. Chem. Phys.* **98**, 5648 (1993).
10. H. Iikura, T. Tsuneda, T. Yanai, and K. Hirao, *J. Chem. Phys.* **115**, 3540 (2001).
11. T. Yanai, D. P. Tew, and N. C. Handy, *Chem. Phys. Lett.* **393**, 51 (2004).
12. M. J. Peach, P. Benfield, T. Helgaker, and D. J. Tozer, *J. Chem. Phys.* **128**, 044118 (2008).
13. P. Hohenberg and W. Kohn, *Phys. Rev.* **136**, B864 (1964).
14. M. Levy, *Proc. Natl. Acad. Sci. USA* **76**, 6062 (1979).
15. E. H. Lieb, *Int. J. Quantum Chem.* **24**, 243 (1983).
16. W. Kohn and L. J. Sham, *Phys. Rev. A* **140**, 1133 (1965).
17. A. D. Becke, *J. Chem. Phys.* **98**, 1372 (1993).
18. J. Toulouse, A. Savin, and H. J. Flad, *Int. J. Quantum Chem.* **100**, 1047 (2004).

19. S. Pazziani, S. Moroni, P. Gori-Giorgi, and G. B. Bachelet, *Phys. Rev. B* **73**, 155111 (2006).
20. J. Toulouse, P. Gori-Giorgi, and A. Savin, *Theor. Chem. Acc.* **114**, 305 (2005).
21. P. Gori-Giorgi and A. Savin, *Phys. Rev. A* **73**, 032506 (2006).
22. P. Gori-Giorgi and A. Savin, *Int. J. Quantum Chem.* **109**, 1950 (2009).
23. J. G. Ángyán, *Phys. Rev. A* **78**, 022510 (2008).
24. E. Fromager and H. J. Aa. Jensen, *J. Chem. Phys.* **135**, 034116 (2011).
25. W. Yang, *J. Chem. Phys.* **109**, 10107 (1998).
26. A. Savin, F. Colonna, and R. Pollet, *Int. J. Quantum Chem.* **93**, 166 (2003).
27. A. M. Teale, S. Coriani, and T. Helgaker, *J. Chem. Phys.* **133**, 164112 (2010).
28. M. D. Strømsheim, N. Kumar, S. Coriani, E. Sagvolden, A. M. Teale, and T. Helgaker, *J. Chem. Phys.* **135**, 194109 (2011).
29. A. M. Teale, S. Coriani, and T. Helgaker, *J. Chem. Phys.* **130**, 104111 (2009).
30. A. M. Teale, S. Coriani, and T. Helgaker, *J. Chem. Phys.* **132**, 164115 (2010).
31. J. Toulouse, P. Gori-Giorgi, and A. Savin, *Int. J. Quantum Chem.* **106**, 2026 (2006).
32. K. Aidas, C. Angeli, K. L. Bak, V. Bakken, R. Bast, L. Boman, O. Christiansen, R. Cimraglia, S. Coriani, P. Dahle, et al., *WIREs Comput. Mol. Sci.* (2013), URL <http://dx.doi.org/10.1002/wcms.1172>.
33. T. H. Dunning Jr., *J. Chem. Phys.* **90**, 1007 (1989).
34. R. A. Kendall, T. H. Dunning Jr., and R. J. Harrison, *J. Chem. Phys.* **96**, 6796 (1992).
35. D. E. Woon and T. H. Dunning Jr., *J. Chem. Phys.* **98**, 1358 (1993).
36. D. E. Woon and T. H. Dunning Jr., *J. Chem. Phys.* **100**, 2975 (1994).

37. J. Koput and K. A. Peterson, *J. Phys. Chem. A* **106**, 9595 (2002).
38. A. K. Wilson, D. E. Woon, K. A. Peterson, and T. H. Dunning Jr., *J. Chem. Phys.* **110**, 7667 (1999).
39. J. Toulouse, W. Zhu, J. G. Ángyán, and A. Savin, *Phys. Rev. A* **82**, 032502 (2010).
40. T. van Mourick and R. J. Gdanitz, *J. Chem. Phys.* **116**, 9620 (2002).
41. J. Stärk and W. Meyer, *Chem. Phys. Lett.* **258**, 421 (1996).
42. E. Fromager, R. Cimiraglia, and H. J. Aa. Jensen, *Phys. Rev. A* **81**, 024502 (2010).
43. S. M. O. Souvi, K. Sharkas, and J. Toulouse, *J. Chem. Phys.* **140**, 084107 (2014).
44. K. Sharkas, A. Savin, H. J. Aa. Jensen, and J. Toulouse, *J. Chem. Phys.* **137**, 044104 (2012).
45. J. K. Pedersen, Ph.D. thesis, University of Southern Denmark (2004).
46. E. Fromager, J. Toulouse, and H. J. Aa. Jensen, *J. Chem. Phys.* **126**, 074111 (2007).
47. E. Fromager, F. Réal, P. Wählin, U. Wahlgren, and H. J. Aa. Jensen, *J. Chem. Phys.* **131**, 054107 (2009).
48. J. Toulouse, F. Colonna, and A. Savin, *Phys. Rev. A* **70**, 062505 (2004).
49. S. N. Steinmann, C. Piemontesi, A. Delachat, and C. Corminboeuf, *J. Chem. Theory Comput.* **8**, 1629 (2012).
50. K. T. Tang and J. P. Toennies, *J. Chem. Phys.* **118**, 4976 (2003).
51. I. Røeggen and L. Veseth, *Int. J. Quantum Chem.* **101**, 201 (2005).
52. W. J. Balfour and A. E. Douglas, *Can. J. Phys.* **48**, 901 (1970).
53. G. C. Lie and E. Clementi, *J. Chem. Phys.* **60**, 1288 (1974).

Figure 1: Interaction energy curves obtained at the CAM-DH*lr*-LDA level for He₂ (a), Ne₂ (b) and Ar₂ (c) with $\mu = 0.4$, $\alpha = 0.19$ and $\beta = 0.46$. Comparison is made with RSDHf-LDA and MP2-srLDA results. Various contributions to the CAM-DH*lr*-LDA interaction energy are also plotted. See text for further details. CAM-DH and RSDHf are here shorthand notations for CAM-DH*lr*-LDA and RSDHf-LDA, respectively. The experimental curves are from Ref.⁵⁰

Figure 2: CAM-DH*lr*-LDA interaction energy curves obtained for He₂ (a), Ne₂ (b) and Ar₂ (c) with $\alpha = 0.2, \beta = 0.7$ and $\alpha = 0.6, \beta = 0.3$. The μ parameter was set to $0.4a_0^{-1}$. Comparison is made with experiment⁵⁰. RSDHf is here shorthand for RSDHf-LDA.

Figure 3: Short-range LDA correlation energy contribution to the interaction energy of He₂ obtained for three bond distances when varying μ with fixed HF-srLDA ($\mu = 0.4$) densities. See text for further details.

Figure 4: Interaction energy curves obtained at the d μ -CAM-DH*lr*-LDA level for He₂ (a), Ne₂ (b) and Ar₂ (c) with $\mu = 0.4$, $\alpha = 0.19$ and $\beta = 0.46$. Comparison is made with CAM-DH*lr*-LDA (using the same parameters) and experiment⁵⁰. d μ -CAM-DH and CAM-DH are here shorthand notations for d μ -CAM-DH*lr*-LDA and CAM-DH*lr*-LDA, respectively.

Figure 5: Interaction energy curves obtained at the CAM-DH*lr*-LDA and d μ -CAM-DH*lr*-LDA levels for Be₂ (a) and Mg₂ (b) with $\mu = 0.4$. Comparison is made with RSDHf-LDA (simply denoted RSDHf here) and MP2-srLDA results. Various contributions to the CAM-DH*lr*-LDA interaction energy are also plotted. d μ -CAM-DH and CAM-DH are here shorthand notations for d μ -CAM-DH*lr*-LDA and CAM-DH*lr*-LDA, respectively. The accurate curves are from Refs.^{51,52} See text for further details.

Figure 6: Total energy curves obtained at the CAM-DH*lr*-LDA and $d\mu$ -CAM-DH*lr*-LDA levels for H₂ (a), Li₂ (b), C₂ (c), N₂ (d) and F₂ (e) with $\mu = 0.4$. $d\mu$ -CAM-DH and CAM-DH are here shorthand notations for $d\mu$ -CAM-DH*lr*-LDA and CAM-DH*lr*-LDA, respectively. Comparison is made with RSDHf-LDA (simply denoted RSDHf here) and MP2-srLDA results. The accurate curves are from Ref.⁵³ See text for further details.

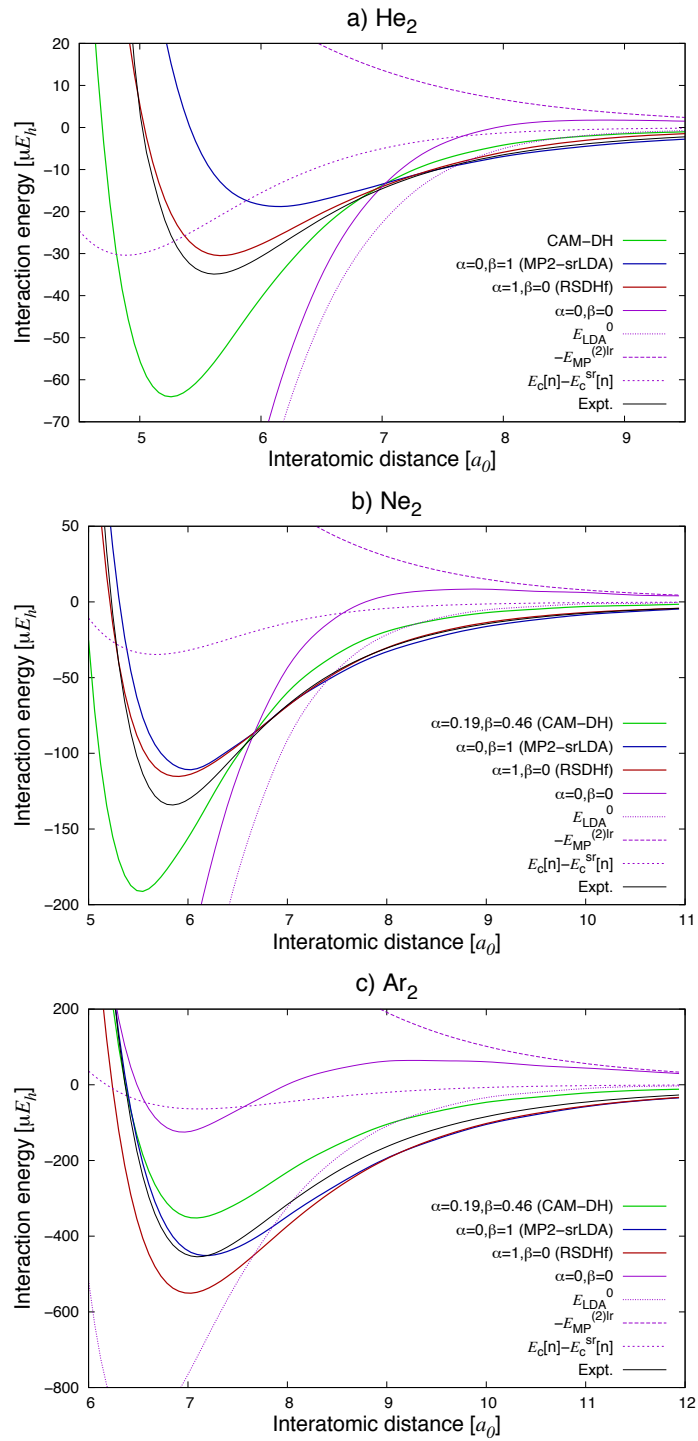


Figure 1
 Yann Cornaton, Emmanuel
 Fromager
 Int. J. Quant. Chem.

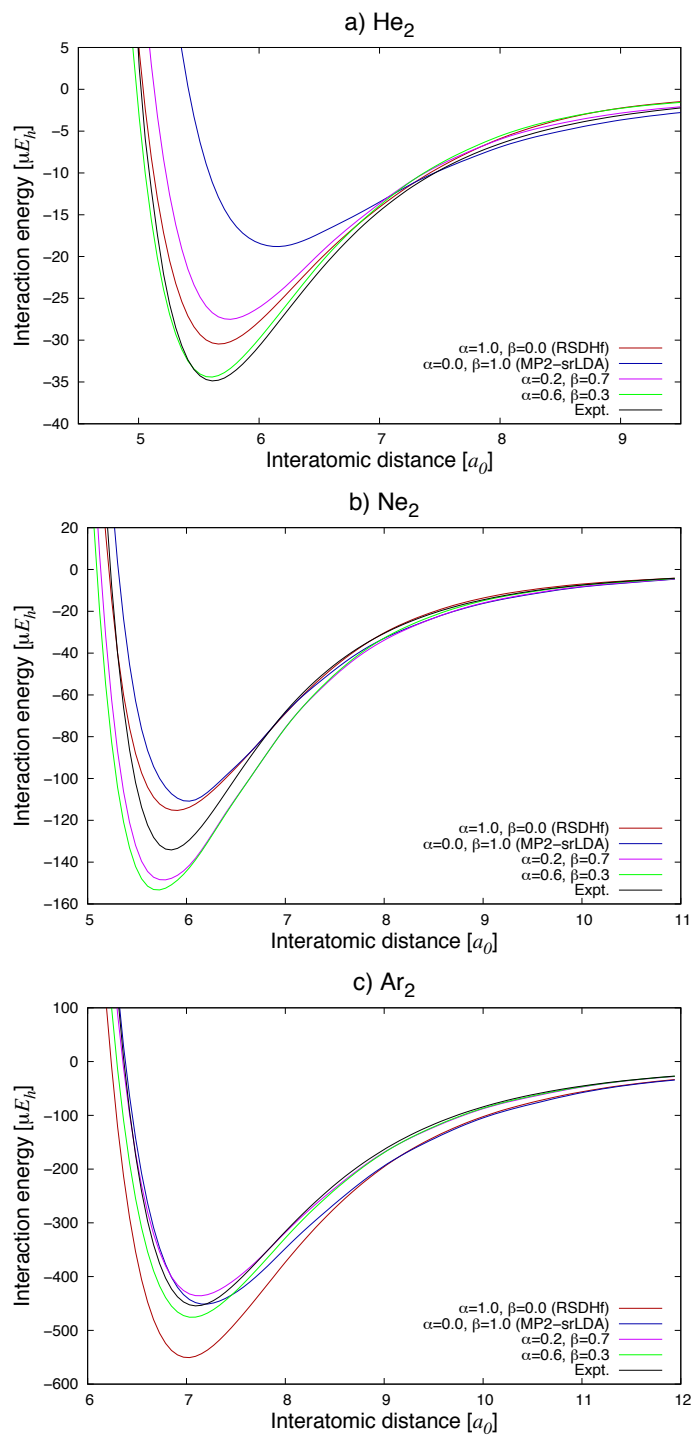


Figure 2
 Yann Cornaton, Emmanuel
 Fromager
 Int. J. Quant. Chem.

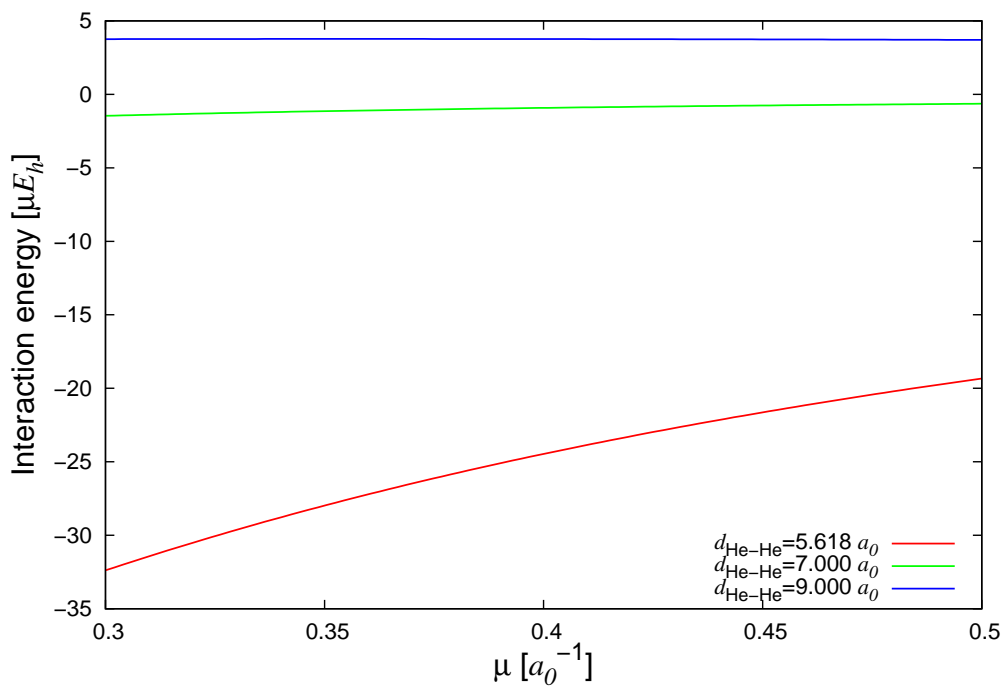


Figure 3
 Yann Cornaton, Emmanuel
 Fromager
 Int. J. Quant. Chem.

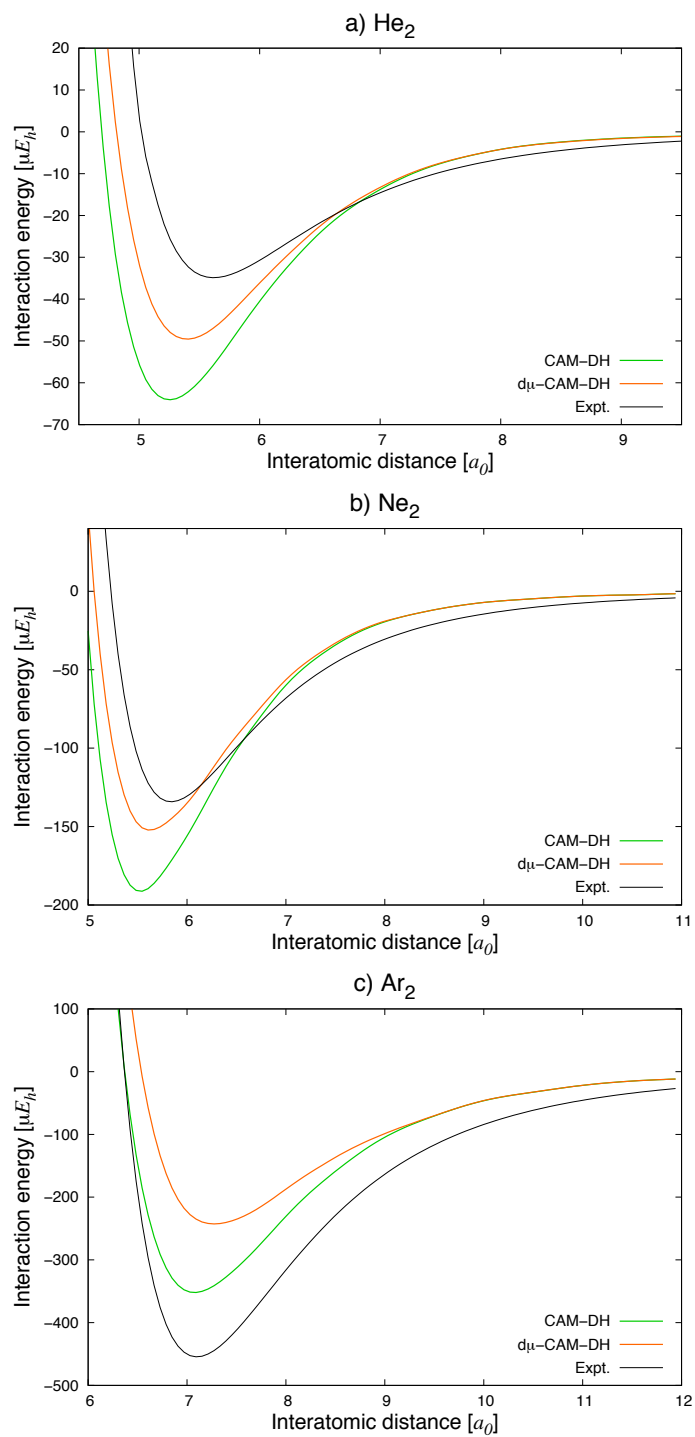


Figure 4
 Yann Cornaton, Emmanuel
 Fromager
 Int. J. Quant. Chem.

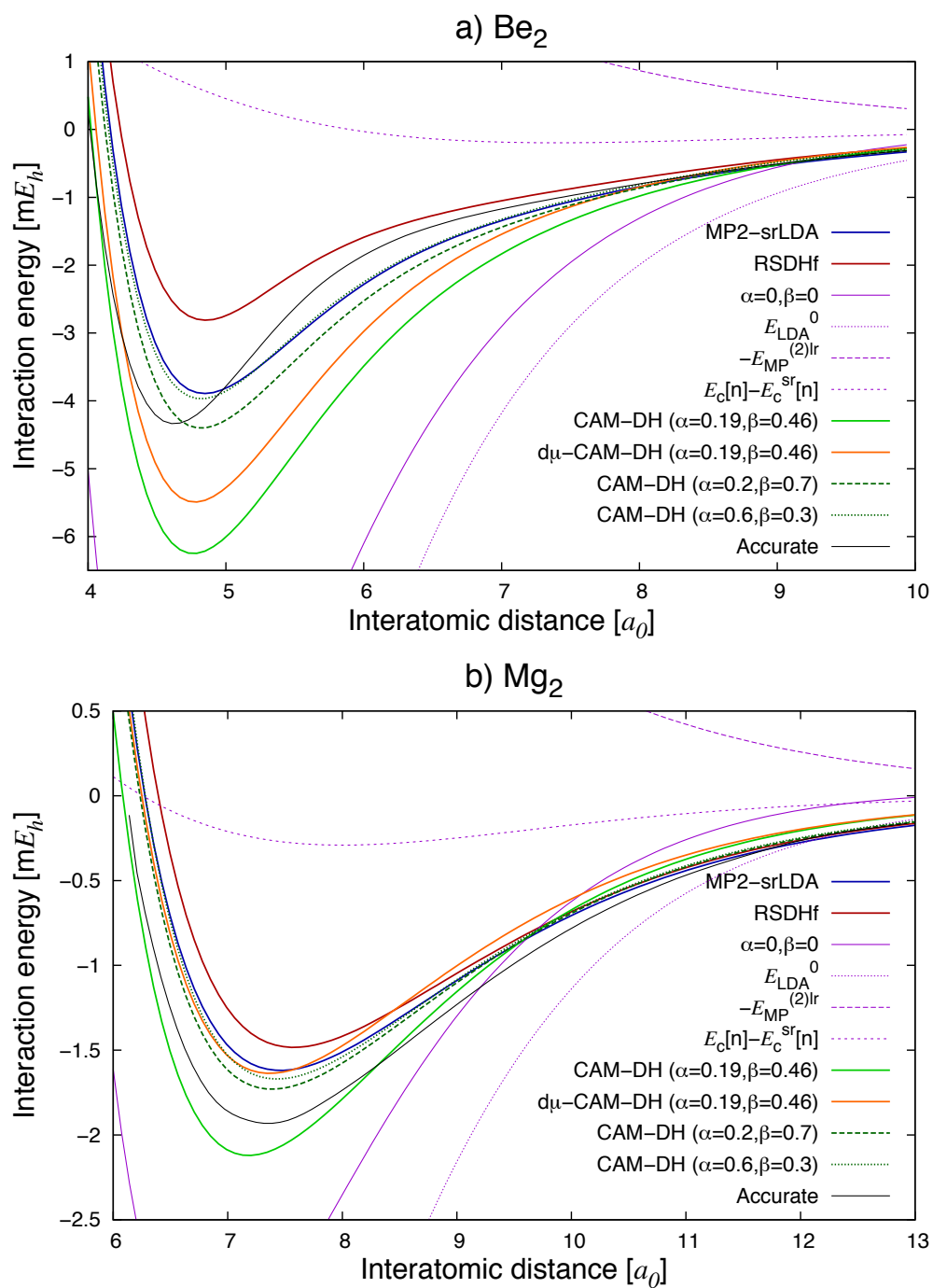


Figure 5
Yann Cornaton, Emmanuel Fromager
Int. J. Quant. Chem.

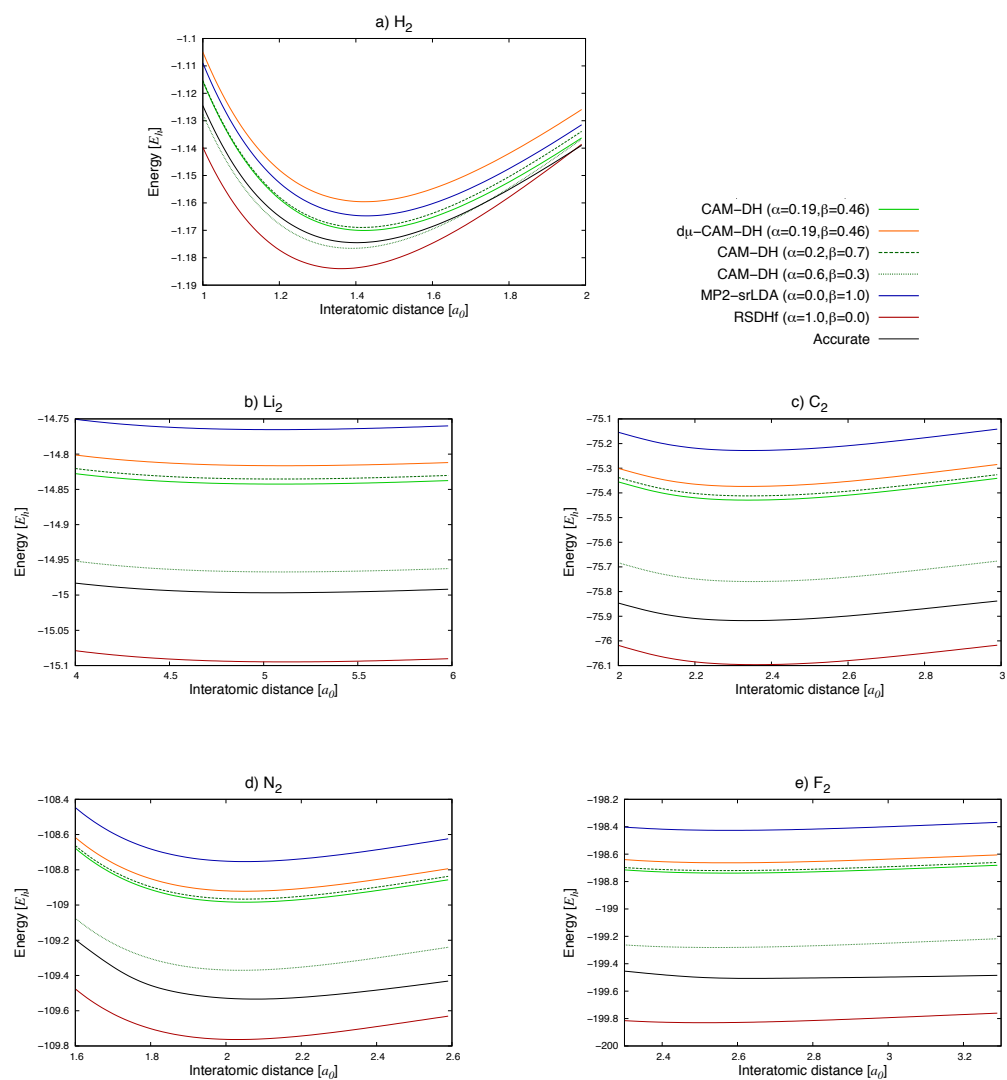


Figure 6
 Yann Cornaton, Emmanuel Fromager
 Int. J. Quant. Chem.